SECOND EUROPEAN CONFERENCE ON EARTHQUAKE ENGINEERING AND SEISMOLOGY, ISTANBUL AUG. 25-29, 2014

SEISMIC RELIABILITY OF BASE-ISOLATED STRUCTURES WITH FRICTION PENDULUM ISOLATORS (FPS)

Bruno PALAZZO[1], Paolo CASTALDO[2] and Pasquale DELLA VECCHIA[3]

ABSTRACT

The friction pendulum system (FPS) is becoming a widely used technique for seismic protection and retrofit of buildings, bridges and industrial structures due to its remarkable features such as the stability of physical properties and durability respect to the elastomeric bearings. Experimental data also showed that the coefficient of friction depends on several effects (i.e., sliding velocity, apparent pressure, air temperature, cycling effect) so that it can be assumed as a random variable. The aim of the study consists in evaluating the seismic reliability of base-isolated structures with FP isolators considering both isolator properties (i.e., coefficient of friction) and earthquake main characteristics as random variables. Assuming appropriate density probability functions for each random variable and adopting the LHS method for random sampling, the input data set has been defined. Several 3D non-linear dynamic analysis have been performed considering both the vertical and horizontal components of each seismic excitation to evaluate the system response. In particular, monovariate and multivariate probability density and cumulative distribution functions have been defined and, considering the limit state thresholds and domains defined respectively on mono/bi-directional displacements, assumed as earthquake damage parameter (EDP) according to performance-based seismic design, the exceeding probabilities have been evaluated. Estimating the reliability of the superstructure, substructure and isolation level led to define a reliability-based abacus to design the FP system.

INTRODUCTION

The friction pendulum system (FPS) is becoming a widely used technique for seismic protection and retrofit of buildings, bridges, and industrial structures due to its remarkable features such as the stability of physical properties and durability respect to the elastomeric bearings (Su et al., 1989). Moreover, other advantages are the separation between the restoring and dissipating action, the better control of the fundamental vibration period and the large deformation capacity by using simple geometric forms.

Studies on controllable seismic isolation systems are usually developed through deterministic analysis in which the isolation system characteristics, structural system properties, earthquake characteristics, and device properties are not random variables and the inherent uncertainties in these systems are not taken into account. Over the years, probabilistic analysis in structural dynamics, structural reliability methods, and reliability based analysis may also contribute to the development of the field. Within the passive seismic control, several reliability analyses through Monte Carlo simulations have been developed on structural systems equipped with different device configurations.

[1] Professor, University of Salerno, Fisciano (SA), palazzo@unisa.it
[2] Research Assistant, University of Salerno, Fisciano (SA), pcastaldo@unisa.it
[3] Graduate Student, University of Salerno, Fisciano (SA), p.dellavecchia@studenti.unisa.it

Specifically, the stochastic responses of base-isolated structures under random earthquake excitations also considering uncertainties related to device properties have been investigated by Fan and Ahmadi (1999), Constantinou and Papageorgiou (1990), Alhan and Gavin (2005).

With reference to isolated system with FP bearings, the inherent uncertainties of the sliding friction coefficient at different velocities, overall structural properties and earthquake characteristics can significantly affect the dynamic response and, therefore, the abovementioned uncertainties should be considered in the dynamical analyses using random variables. The aim of the study consists in evaluating the seismic reliability of an ordinary base-isolated structure through FP isolators with a design life of 50 years and located in Italy, considering both earthquake main characteristics (i.e., spectral response acceleration at the isolated structural period) and isolator properties (i.e., sliding friction coefficient) as random variables by evaluating the exceeding probabilities of displacement limits as provided by performance-based seismic design (PBSD) (SEAOC Vision 2000, 1995). In particular, normal and uniform density probability functions have been assumed according, respectively, to seismic hazard at the specific site as provided by NTC08 (2008) and experimental tests (Mokha et al. 1990; Constantinou et al. 1990). Adopting the LHS method (McKay et al., 1979) for random sampling, the input data set has been defined to perform several 3D non-linear dynamic analyses in order to evaluate the system response considering both the vertical and horizontal components of each seismic excitation. Monovariate and multivariate probability density and cumulative distribution functions have been defined and, considering the limit state thresholds and domains defined respectively on mono/bi-directional displacements, assumed as earthquake damage parameter (EDP) according to performance-based seismic design (SEAOC Vision 2000, 1995), the exceeding probabilities have been evaluated. The reliability evaluation related to the superstructure, substructure and isolation level led to define a reliability-based abacus useful to design the FP system.

SEISMIC RELIABILITY AND PERFORMANCE OBJECTIVES

Seismic reliability assessment of a building structure, according to the structural performance evaluation method (Collins and Stojadinovic, 2000; Bertero and Bertero, 2002; Aoki et al., 2000), is based on the coupling of structural performance levels (SEAOC Vision 2000, 1995) and associated reliability indices β or exceeding probabilities during its design life (CEN, 2006; Saito et al., 1998). As for performance levels of a building, defined in terms of measurable structural response parameter IDI, Interstory Drift Index, four discrete performance levels, or limit states (*LS1*, *LS2*, *LS3*, *LS4*), corresponding respectively to “fully operational”, “operational”, “life safety” and “collapse prevention” are assumed (SEAOC Vision 2000, 1995). Each one of the performance item (Aoki et al., 2000) is related to the acceptable probability of going beyond that limit state, or failure probability, in design life of a structure (Collins and Stojadinovic, 2000; Bertero and Bertero, 2002). In Table.1, with reference to a fixed-base reinforced concrete structure, the limit states with the values of both failure probabilities and reliability indices β in 50 years are reported as provided by the codes (CEN, 2006; Saito et al., 1998). In Fig.1 the corresponding “performance curve” is illustrated.

Table 1. Limit states corresponding to Interstory Drif Indices and Reliability Indices in 50 years (Aoki et al., 2000; Collins and Stojadinovic, 2000; Bertero and Bertero, 2002)

Performance of building	Limit State	Interstory Drift Index (%)	Reliability Index β	P_f
Concrete crack	LS1	0.30	0	$5.0 \cdot 10^{-1}$
Damage on secondary elements	LS2	0.60	1	$1.6 \cdot 10^{-1}$
Failure of structural elements	LS3	1.50	2	$2.2 \cdot 10^{-2}$
Collapse of building	LS4	2.00	3	$1.5 \cdot 10^{-3}$

In the “performance space” (Collins and Stojadinovic, 2000; Bertero and Bertero, 2002), Fig.1, three performance curves are here represented. Starting from the performance levels previously identified, related to fixed-base systems, the performance limit states for a base-isolated building, in accordance to both FEMA (FEMA 274, 1997) and Italian seismic code (NTC 08, 2008) provisions, have been evaluated by limiting the response of the lateral-load-resisting superstructure system, IDI limits, to a fraction of that permitted for designing a comparable fixed-base building. In particular,

with regard to FEMA 274 provisions the limit response of the lateral-load-resisting superstructure system of a base-isolated building is equal to one-third of that of a comparable fixed-base building. Whereas, the Italian seismic code NTC08 (NTC08, 2008) provides an increased value equal to two-third of the one permitted for designing a comparable fixed-base building.

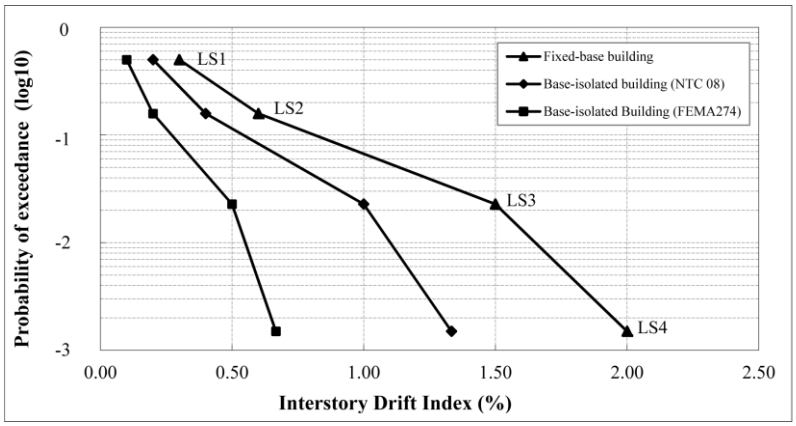

Figure 1. Exceeding probability (in 50 years) of the performance limit states in the "performance space"

The curves, illustrated in Fig.1, are defined as the Performance Objective (PO) curves according to the code provisions. The "safe region" is the space below the PO curves.

FORCE–DISPLACEMENT RELATIONSHIP OF THE SINGLE FP BEARING

Single FP bearings are devices which support vertical load and transmit horizontal loads in a predefined manner trough an articulated slider which slides on a concave surface (Fig.2(a), 2(b)). The behavior of the isolation system, described originally by Zayas et al. (1987), is based on the pendulum motion: the center of the spherical concave plate follows a circular trajectory so that the motion is that of a pendulum having a length equal to the radius of curvature *R*. The bearing could be installed both in upward or downward position.

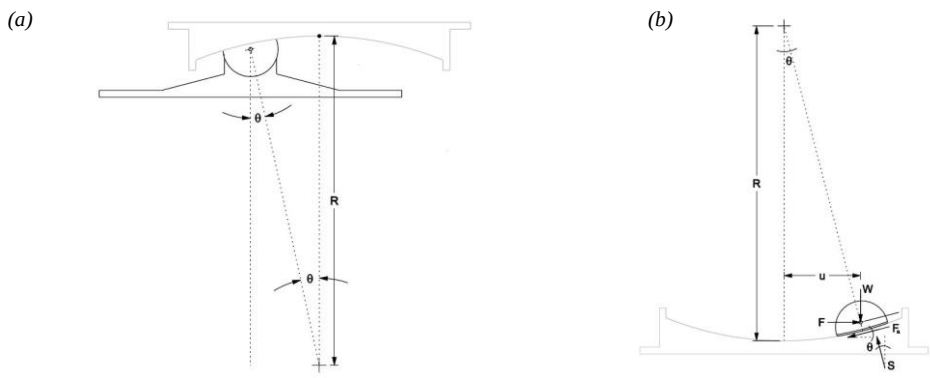

Figure 2. Pendulum motion and geometry illustration (bearing in upward position) (a); acting forces on the FP bearing (bearing in downward position) (b)

From the equilibrium of forces acting on the bearing in the vertical and horizontal directions, Fig.2(b), the force-displacement relationship, that governs the motion of the FP bearing, results being Eq.(1):

$$F = \frac{W}{R}u + \mu W \operatorname{sgn}(\dot{u}) \tag{1}$$

where u is the horizontal displacement of the pivot point of the slider, *sgn* denotes the signum function of the sliding velocity $\dot{u}$, R is the radius of curvature of the spherical surface, W is the weight on the bearing and μ is the coefficient of sliding friction, variable with several factors, in particular sliding velocity and pressure (Mokha et al., 1990). The resisting force F is sum of the pendulum component, direct towards the center bearing, and of the friction component, acting in opposite direction of istantaneous velocity. The fundamental period of vibration of the system, T, related only to pendulum component, is independent of the mass of the structure and related only to the radius of curvature of the spherical surface R, Eq.(2):

$$T = 2\pi\sqrt{R/g} \tag{2}$$

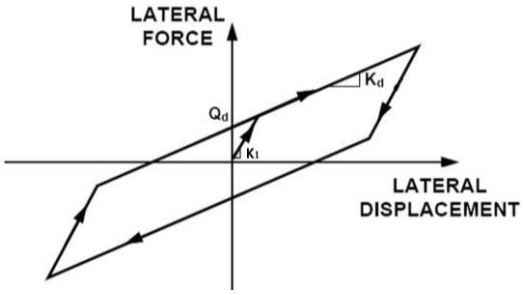

Figure 3. Bilinear force-displacement relationship

The FP bearings can also be modeled by a bilinear hysteretic model (Naeim and Kelly, 1999) (Fig.3) with characteristic strength given by $Q_d=\mu W$; the post-elastic stiffnes can be determined as $K_d=W/R$; the elastic stiffness K_1 should be at least 51 times larger than the post-elastic stiffnerss K_d (Naeim and Kelly, 1999). The mathematical model of the velocity dependence of the friction coefficient for a given bearing pressure, is the one proposed by Constantinou et al. (1990), in accordance with experimental results, Eq.(3):

$$\mu = f_{\max} - (f_{\max} - f_{\min})\exp(-a\dot{u}) \tag{3}$$

where f_{max} and f_{min} are the sliding coefficients of friction at large velocity and nearly zero sliding velocity respectively, and a, selected on the basis of available experimental results, is a parameter that controls the transition of the coefficient of friction from the its minimum to its maximum value.

BASE-ISOLATED STRUCTURAL MODEL

A 3-D 4-story symmetric RC frame building has been considered for the analyses as a benchmark model of a base-isolated structure (Almazàn and De la Llera, 2003). The superstructure and substructure are, respectively, composed of three and one stories. A FEM model, Fig.4, has been defined in SAP2000 (CSI, 2002): the plan dimensions of the structure are 8.0 x 16.0 m with slabs having a depth of 0.4 m; the interstory heights of the substructure and superstructure are, respectively, 3.0 m and 3.5 m; substructure and superstructure column section dimensions are 0.8 x 0.8 m and 0.7 x 0.7 m, respectively; beam section dimensions are 0.40 x 0.70 m for each floor level. Each floor has been modeled as diaphragm and assumed to be rigid in its own plane, so that at each floor level three degrees of freedom resulted: two lateral degrees of freedom in the x and y directions, and a rotational degree of freedom (ϑ) around the vertical axis. Considering a seismic weight w_s=1.0 tm^{-2} at each level, the total weight of the superstructure is W_s=512.0 t. The FP isolation bearings, are located on top of the substructure columns; the curvature radius, R=1.50 m, is selected to exhibit a pendulum period equal to 2.58 s (Eq.2). The isolators are modeled using the non-linear link "Friction Pendulum" elements allowing only compression behavior along the vertical direction, and having coupled frictional properties in the two horizontal directions. The shearing behavior is based on the model proposed by Park et al. (1986) and extended for seismic isolation bearings by Nagarajaiah et al.

(1991). As discussed in previous section, the mathematical model of the frictional behavior with the dependence of the friction on both sliding velocity and bearing pressure, the linear and non-linear properties have been properly provided in order to perform non-linear time history analyses. Developing the eigenvalue analysis, the first natural period of the fixed-base structure results being T=0.54 s, while for the base-isolated structure T_{is}=2.58 s. A proportional Rayleigh damping, through Eq.(4), has been assumed and, setting the damping of the first two modes equal to 2%, mass proportional α and stiffness proportional β coefficients result being equal to 0.0244 and 0.0041, respectively.

$$C = \alpha M + \beta K \tag{4}$$

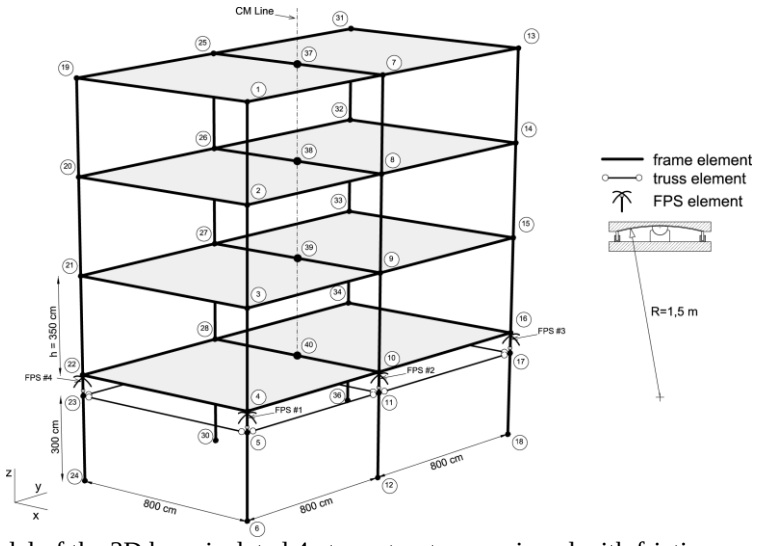

Figure 4. Structural model of the 3D base-isolated 4-story structure equipped with friction pendulum system (modified from Almazàn and De la Llera, 2003)

RANDOM VARIABLES AND SAMPLING METHOD

Seismic reliability assessment of the considered base-isolated structure through FP isolators, with a design life of 50 years and located in L'Aquila (Italy), has been performed with regard to the following two random variables: isolator properties (i.e., sliding friction coefficient) and earthquake main characteristics (i.e., spectral response acceleration at the isolated structural period). With reference to the friction coefficient, the experimental data, developed by Mokha et al. (1990) and Constantinou et al. (1990), have pointed out that friction is a complex phenomenon, not complying with the Coulomb friction law (friction constant during sliding) and that several mechanisms contribute to its variability, such as:

1. Coefficient of sliding friction increases with the sliding velocity approximately from 5 to 6 times, starting from a minimum value f_{min} to a maximum value f_{max}, reached at speeds of seismic interest (500mm/s or larger);
2. Increases in the apparent pressure result in reduction of the coefficient of friction and the rate of reduction is almost insensitive to sliding velocity and air temperature;
3. Variations in the temperature (from 50°C to minus 40°C), affect the values of static and low velocity sliding coefficient of friction by approximately a 7-fold increase in the values, due to changing viscoelastic properties of sliding materials, while the frictional heating that occurs at large velocities of sliding moderates the effect of low temperature;
4. Lower sliding friction (of both high and low velocity) greater number of cycles at high speeds due to the effects of frictional heating of the interfaces;
5. The effect of specimen size affects the value of coefficient of friction (very large specimens exhibit slightly lower values).

Taking into account the above studies, a uniform density probability function, ranging from 3% to 15%, has been assumed for the sliding friction random variable. The uncertainty of ground motion has been taken into account, according to seismic hazard provided by NTC08 (NTC, 2008), assuming the spectral acceleration ($S_a(T_{is})$) as a random variable. The probabilistic seismic hazard analysis (PSHA) (Cornell, 1968) considers *lnPGA*[g] or lnS_a[g] as a random variable characterized by a Gaussian probability density function (PDF) to evaluate the occurrence rate of an earthquake having that intensity measure in 1yr. The exceeding probabilities related to different intensity measures, limit states (*SLO, SLD, SLV, SLC*), are provided by NTC08 (NTC08, 2008) for each Italian site and design life. Indeed, with reference to L'Aquila site (Italy), design life of 50 years and dimensionless damping coefficient equal to 5%, Fig.5(a) shows the design spectral response accelerations related to the different limit states. With the aim to consider the abovementioned uncertainty, a Gaussian PDF of the lnS_a[g] random variable corresponding to the fundamental period ($T_{is}=2.58$ *s*) of the isolated structure (Fig.5(b)) has been defined having a mean $lnS_a(T_{is})$[g] and COV equal to -3.83 and 16%, respectively.

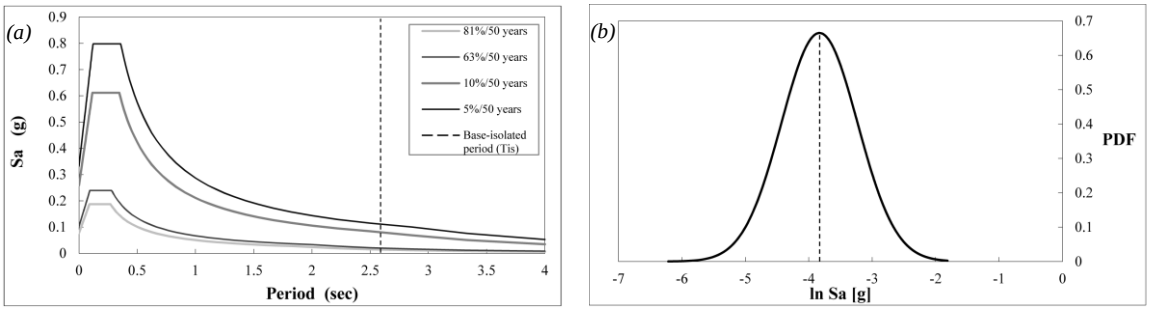

Figure 5. Design spectral response acceleration (ξ=5%), L'Aquila site (Italy) (*a*); normal distribution of the seismic intensity referred to the fundamental period (*T=2.58 s*) of the isolated study structure (*b*).

Defined both the PDFs and assuming that the two random variables are independent and uncorrelated, it has been fundamental to choose an appropriate sampling method providing adequate accuracy of the results, even for a small sample size. The stratified sampling method Latin hypercube sampling (LHS) proposed by McKay et al. (1979), is a technique based on both the variance reduction and stratified sampling, making the inputs to simulations more regular than random inputs. Each one of the two probability density functions, $i=2$, has been divided in $j=22$ non overlapping intervals on the basis of equal probability. Each random variable Y_i is sampled by using N_{Sim} values. The *j*-th sample value of the *i*-th random variable Y_i can be obtained through Eq.(5):

$$y_{j,i} = F_i^{-1}(p_{j,i}) = F_i^{-1}\left(\frac{\pi_i(j)-0.5}{N_{Sim}}\right) \qquad \begin{array}{l} i=1,\ldots,N_{\text{var}}, \\ j=1,\ldots,N_{Sim}, \end{array} \tag{5}$$

where $p_i(j)$ is a random permutation of $1, \ldots, N_{Sim}$, $p_{i,j}$ is the probability that the random variable Y_i is less than or equal to $y_{j,i}$, and F_i^{-1} is the inverse of the cumulative distribution function (CDF) of the random variable Y_i, evaluated at the probability $p_{j,i}$. More details about the LHS technique and its application can be found elsewhere (e.g. in Dolsek, 2009; Vořechovský and Novák, 2009; Celarec and Dolšek, 2013). The sample of random values is then used to generate a set of N_{Sim} structural models, which reflect the modeling uncertainties, so that the set represents the probabilistic structural model. Being a uniform distribution the PDF of the friction coefficient, each random value selected from each one of the 22 intervals of the friction coefficient r. v. has been paired to each one of the other r. v.: a set of a total number of simulations equal to $j^i=484$ has been obtained and used as input data for the non-linear dynamic time-history analyses. In order to employ unscaled historical records with the three components, the selection from the European Strong-Motion Data Base (ESMD) has been developed with reference to a horizontal component, in order to reproduce the random selection of the 22 spectral accelerations $S_a(T_{is}$=2.58 s) of the isolated structure obtained from the LHS method. Fig.6(a) and Fig.6(b) show the acceleration spectra corresponding to the selected unscaled historical earthquake excitations, for x and y directions, respectively. The ground motion records have been selected by

imposing a magnitude and epicentral distance raging, respectively, between $5 < M < 7$ and $0 < R < 30$ km. The characteristics of the selected ground motion records are listed in Table.2.

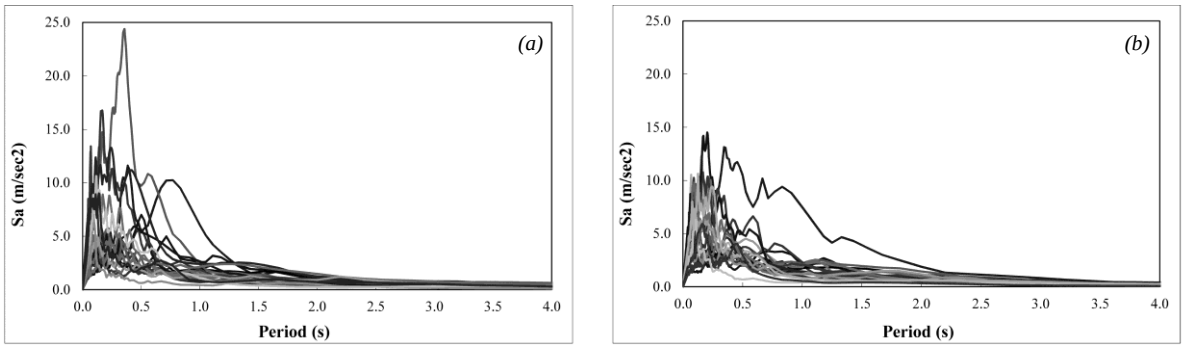

Figure 6. Acceleration spectra (ξ=5%) of the selected ground motion for "L'Aquila" site (Italy): x direction (*a*); y direction (*b*)

Table 2. Selected ground motion records

	Earthquake	Date	M	EC8 Site class	Waveform ID	Earthquake ID
GM1	Bingol	2003_May_01	6.3	B	209	38
GM2	Christchurch	2011_June_13	6	A	386	149
GM3	Darfield	2010_September_03	7.1	C	330	137
GM4	E Off Izu Peninsula	1998_May_03	5.5	B	153	59
GM5	EMILIA_Pianura_Padana	2012_May_29	6	C	313	133
GM6	Friuli 4th shock	1976_September_15	5.9	B	429	75
GM7	Hector Mine	1999_October_16	7.1	B	412	35
GM8	Honshu	1996_August_10	5.9	B	56	21
GM9	Hyogo - Ken Nanbu	1995_January_16	6.9	C	306	34
GM10	Landers	1992_June_28	7.3	B	457	98
GM11	L'Aquila mainshock	2009_April_06	6.3	B	167	64
GM12	Loma Prieta	1989_October_18	6.9	B	456	94
GM13	Mid Niigata Prefecture	2004_October_23	6.6	C	41	16
GM14	MT FUJI REGION	2011_March_15	5.9	B	285	125
GM15	N Miyagi Prefecture	2003_July_25	6.1	C	34	15
GM16	Northridge	1994_January_17	6.7	C	459	99
GM17	Off Noto Peninsula	2007_March_25	6.7	B	136	50
GM18	Olfus	2008_May_29	6.3	A	218	101
GM19	Rumoi	2004_December_14	5.7	B	47	18
GM20	South Iceland	2000_June_17	6.5	A	113	41
GM21	Southern Iwate Prefecture	2008_June_13	6.9	B	139	51
GM22	W Tottori Prefecture	2000_October_06	6.6	B	20	12

Adopting a single record for each value of S_a means that the record to record dependence has been neglected. This assumption can be accepted as numerical result since the differences in terms of response are negligible due to the high isolated period and hysteretic behavior of the FP bearings able to develop high damping.

SEISMIC RELIABILITY ANALYSIS

Carried out the non-linear dynamic analyses considering the three components of each unscaled record, through the maximum likelihood estimation method, lognormal probability density functions for each horizontal displacement component (*x* and *y* directions) corresponding respectively to each level of the superstructure, isolation system and substructure have been derived through Eq.(6):

$$f(\delta) = \frac{1}{\delta\sigma_{\ln(\delta)}\sqrt{2\pi}} \exp\left[-\frac{1}{2}\left(\frac{\ln(\delta) - \mu_{\ln(\delta)}}{\sigma_{\ln(\delta)}}\right)^2\right] \tag{6}$$

where δ is the random variable, $\mu_{ln(\delta)}$ and $\sigma_{ln(\delta)}$ are, respectively, the mean and standard deviation of $ln(\delta)$. With reference to substructure and superstructure, δ is the interstory drift along x or y direction (δ_x or δ_y); as regards FPS isolators δ is the horizontal displacement on x or y direction (u_x or u_y).

Lognormal monovariate CDFs and PDFs related to both x and y directions of each level are, respectively, shown in Fig.7(a)-11(a) and Fig.7(b)-11(b).

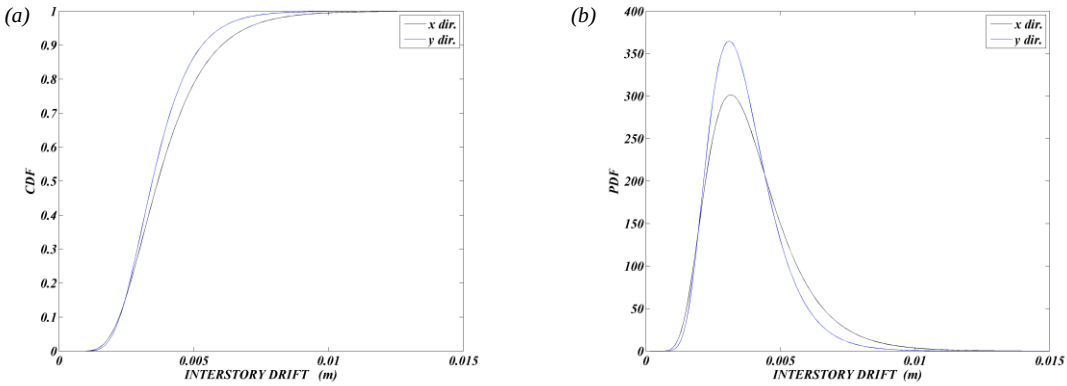

Figure 7. Lognormal monovariate CDFs (a) and PDFs (b) related to interstory drift at 4th story

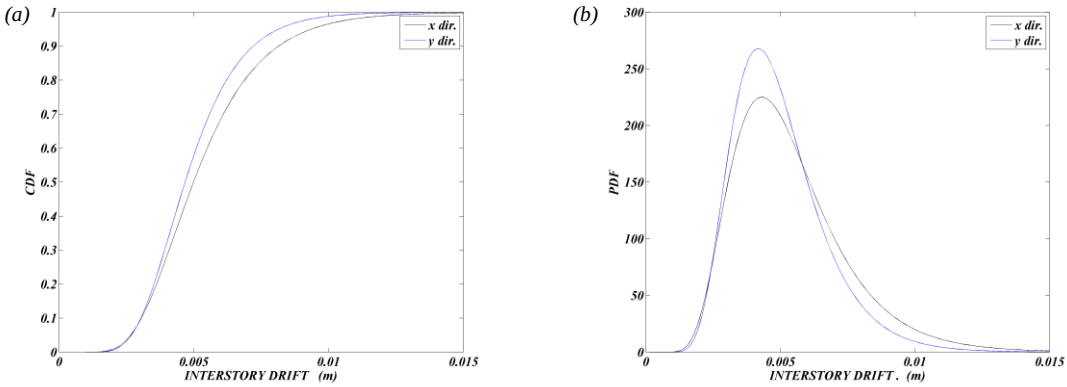

Figure 8. Lognormal monovariate CDFs (a) and PDFs (b) related to interstory drift at 3rd story

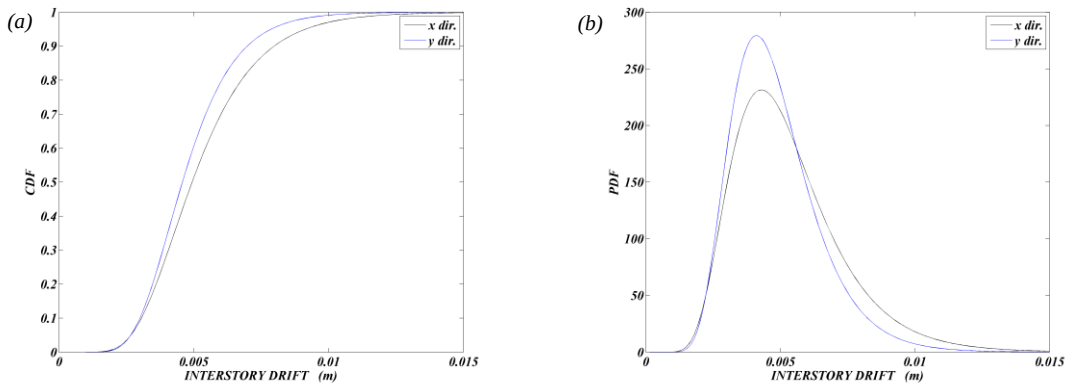

Figure 9. Lognormal monovariate CDFs (a) and PDFs (b) related to interstory drift at 2nd story

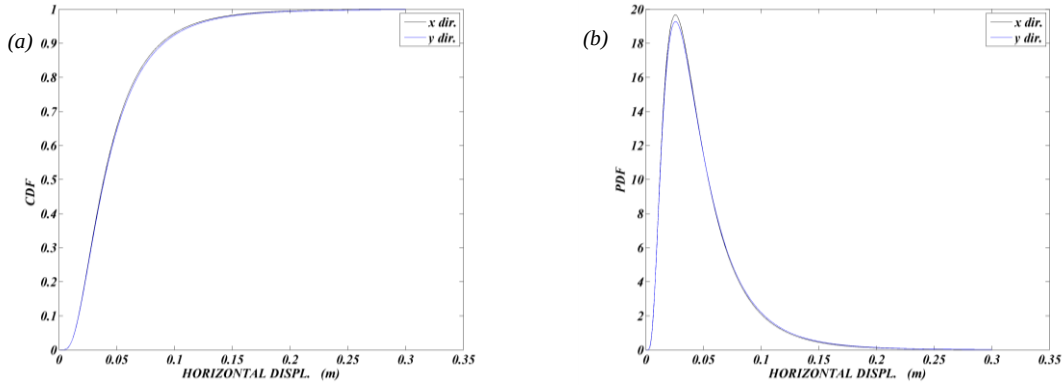

Figure 10. Lognormal monovariate CDFs (a) and PDFs (b) related to FP bearing horizontal displacements

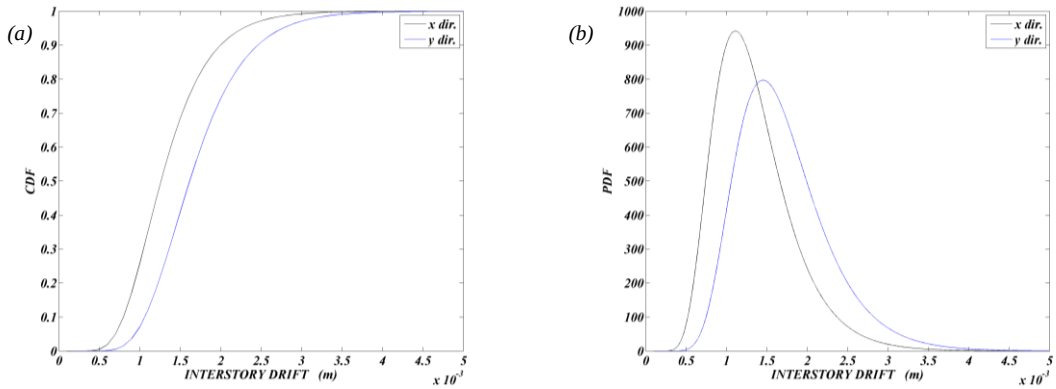

Figure 11. Lognormal monovariate CDFs (a) and PDFs (b) related to interstory drift at 1st story

Similarly, lognormal bivariate probability density functions have been respectively evaluated by estimating the matrix of correlation coefficients, Eq.(7).

$$f(\delta_1,\delta_2)=\frac{1}{2\pi\delta_1\delta_2\sigma_{\ln(\delta_1)}\sigma_{\ln(\delta_2)}\sqrt{1-\rho^2}}\cdot$$
$$\cdot\exp\left\{-\frac{1}{2(1-\rho^2)}\left[\left(\frac{\ln(\delta_1)-\mu_{\ln(\delta_1)}}{\sigma_{\ln(\delta_1)}}\right)^2-2\rho\left(\frac{\ln(\delta_1)-\mu_{\ln(\delta_1)}}{\sigma_{\ln(\delta_1)}}\right)\left(\frac{\ln(\delta_2)-\mu_{\ln(\delta_2)}}{\sigma_{\ln(\delta_2)}}\right)+\left(\frac{\ln(\delta_2)-\mu_{\ln(\delta_2)}}{\sigma_{\ln(\delta_2)}}\right)^2\right]\right\} \quad (7)$$

where δ_1 and δ_2 are the random variables, $\mu_{\ln(\delta_1)}$ and $\mu_{\ln(\delta_2)}$ are their mean values, $\sigma_{\ln(\delta_1)}$ and $\sigma_{\ln(\delta_2)}$ are their standard deviations and ρ is the correlation coefficient. As for substructure and superstructure stories, δ_1 and δ_2 are, respectively, interstory drifts along *x* and *y* directions (δ_x and δ_y); as regards the FPS isolator δ_1 and δ_2 are the horizontal displacement along *x* and *y* directions (u_x and u_y). Considering the limit state domains (Fig.12) defined respectively on the lognormal bivariate probability density functions (Fig.13(a)-17(a)) related to bi-directional displacements, assumed as earthquake damage parameter (EDP) according to performance-based seismic design (SEAOC Vision 2000, 1995), the exceeding probabilities have been evaluated. The different limit state thresholds or functions have been defined in terms of interstory drift and isolation relative displacement in order to estimate the seismic reliability of the system. Fig.13(b)-17(b) show the exceeding probabilities, plotted in logarithmic scale, of each level of the superstructure for different limit domains, defined in terms of IDI (Interstory Drift Index), substructure and isolation system for different displacement limits.

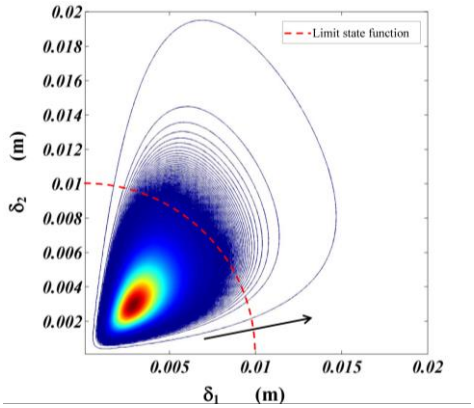

Figure 12. Bivariate limit state function

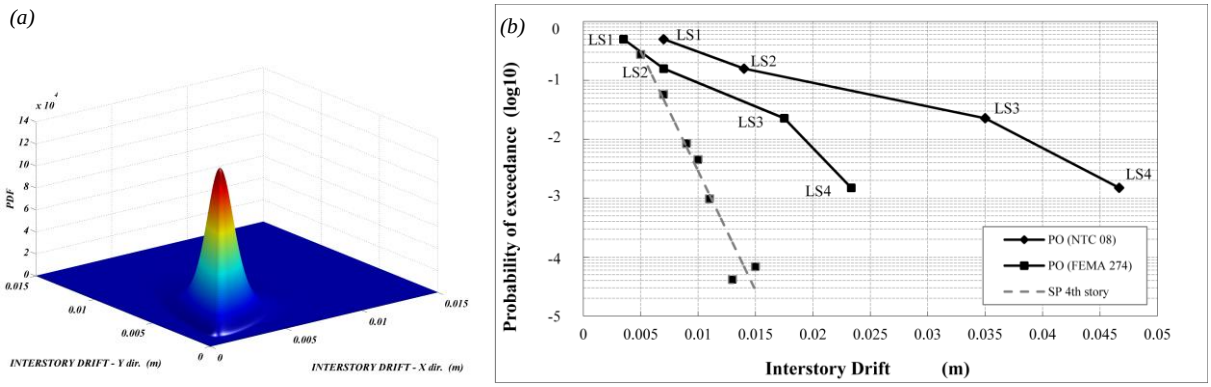

Figure 13. Lognormal bivariate PDF related to interstory drift at 4th story (a); Exceeding probabilities of interstory drift at 4th story for different displacement limits (b)

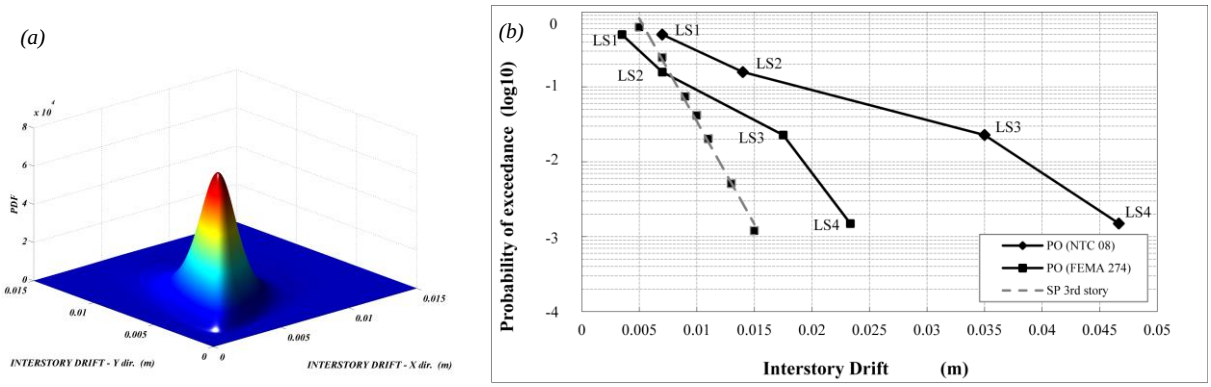

Figure 14. Lognormal bivariate PDF related to interstory drift at 3rd story (a); Exceeding probabilities of interstory drift at 3rd story for different displacement limits (b)

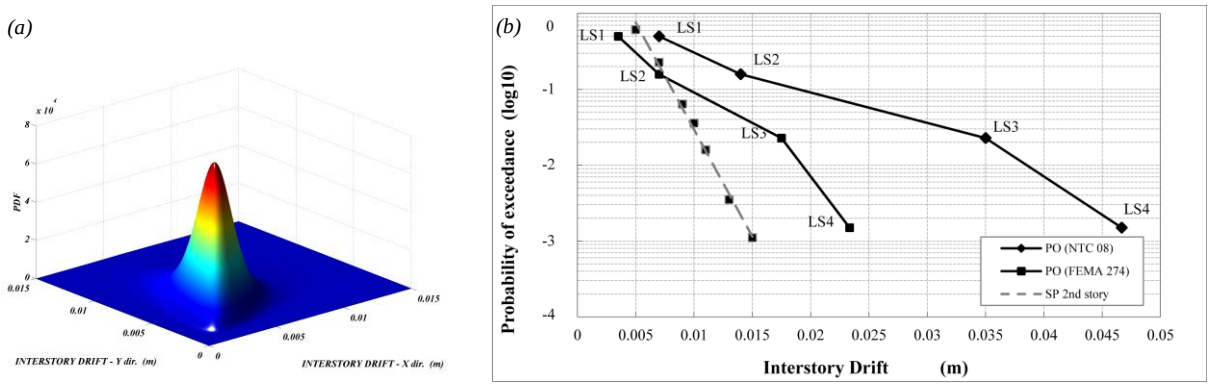

Figure 15. Lognormal bivariate PDF related to interstory drift at 2nd story (a); Exceeding probabilities of interstory drift at 2nd story for different displacement limits (b)

With reference to the performance levels (*LS1, LS2, LS3, LS4*), the structural performance curves of superstructure (*SP 4th story, SP 3rd story, SP 2nd story*) and substructure (*SP 1st story*), fall within the safe region defined on the basis of NTC08 provisions for base-isolated structures. Conversely, with regard to FEMA 274 provisions, the limit states *LS1* and *LS2* are slightly violated at the first two levels of the superstructure. It is possible, from the structural performance curve of the isolation level, ($SP_{isolator}$), (Fig.16(b)), to design the plan dimension of the isolator (i.e. radius in plan of the concave surface) in order to respect the reliability levels. In particular, an exceeding probability of $P_f=1.5\cdot10^{-3}$ (reliability index β=3 in 50 years), could be obtained through a radius in plan of about 0.3 m, corresponding to a plan diameter of the concave surface approximately equal to about 0.6 m.

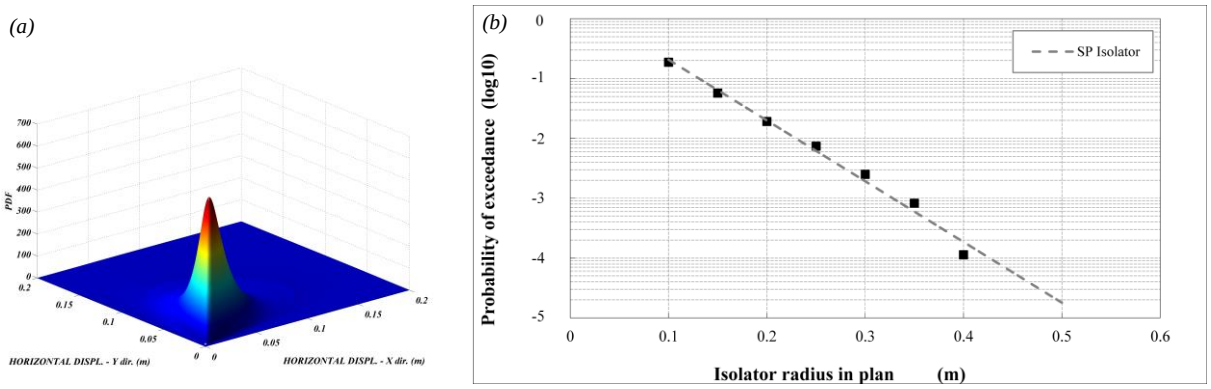

Figure 16. Lognormal bivariate PDF related to FP bearing horizontal displacements (a); Exceeding probabilities (b)

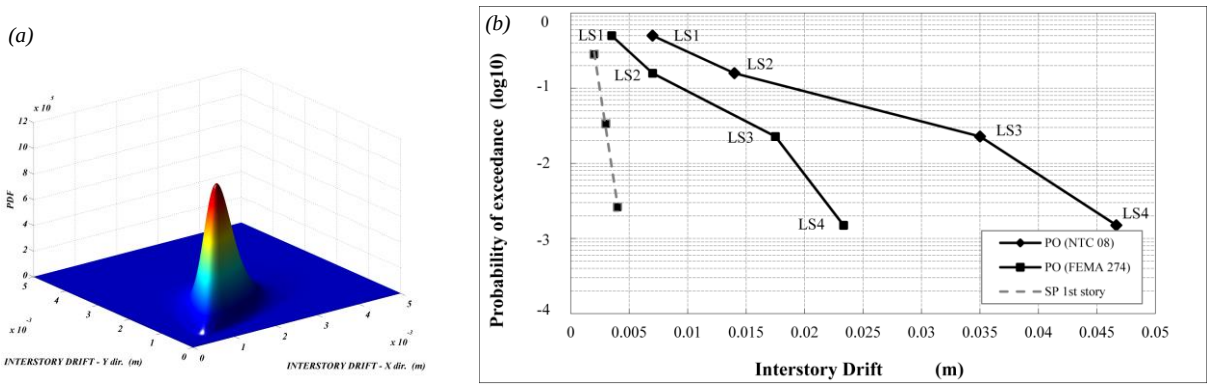

Figure 17. Lognormal bivariate PDF related to interstory drift at 1st story (a); Exceeding probabilities of interstory drift at 1st story for different displacement limits (b)

CONCLUSIONS

The purpose of the study is to evaluate the seismic reliability of an ordinary base-isolated structure through FP isolators with a design life of 50 years and located in L'Aquila (Italy), considering both earthquake main characteristics and isolator properties as random variables. Several 3D non-linear dynamic analyses have been performed in order to evaluate the system response considering both the vertical and horizontal components of each seismic excitation. Monovariate and multivariate probability density and cumulative distribution functions have been computed and, assuming the limit state thresholds and domains defined respectively on mono/bi-directional displacements, the exceeding probabilities have been estimated. Therefore, it has been possible to evaluate the seismic reliability of the system. With reference to the performance levels (*LS1, LS2, LS3, LS4*), the structural performance curves of superstructure (*SP 4th story, SP 3rd story, SP 2nd story*) and substructure (*SP 1st story*), fall within the safe region for base-isolated structures according to NTC08 provisions. Conversely, with regard to FEMA 274 provisions, the limit states *LS1* and *LS2* are slightly violated at the first two levels of the superstructure. Using the structural performance curve of the isolation level,

($SP_{isolator}$), it is possible to design the plan dimension of the isolator (i.e. radius in plan of the concave surface) in order to respect the reliability levels. In particular, an exceeding probability of $P_f=1.5\cdot10^{-3}$ (reliability index β=3 in 50 years), could be obtained through a radius in plan of about 0.3 m, corresponding to a plan diameter of the concave surface approximately equal to about 0.6 m. The seismic reliability evaluation related to the superstructure, substructure and isolation level, allowed to define reliability-based abacus useful to design the FP bearing devices having a radius of curvature R=1.5 m, in an area with a seismic hazard similar to that considered.

REFERENCES

Alhan C, Gavin HP (2005) "Reliability of base isolation for the protection of critical equipment from earthquake hazards", *Engineering Structures*, 27: 1435-1449.

Almazàn JL and De la Llera JC (2003) "Physical model for dynamic analysis of structures with FPS isolators" *Earthquake Engng Struct. Dyn.*, 32:1157–1184 (DOI: 10.1002/eqe.266).

Aoki Y, Ohashi Y, Fujitani H, Saito T, Kanda J, Emoto T, Kohno M (2000) "Target seismic performance levels in structural design for buildings" *12WCEE.*

Bertero RD, Bertero VV (2002) "Performance-based seismic engineering: the need for a reliable conceptual comprehensive approch", *Earthquake Engng Struct. Dyn.*, 31:627–652 (DOI: 10.1002/eqe.146).

Building Seismic Safety Council (1997) "NEHRP commentary on the guidelines for the seismic rehabilitation of buildings. Provisions (FEMA 274). Washington, DC.

Celarec D, Dolšek M (2013) "The impact of modelling uncertainties on the seismic performance assessment of reinforced concrete frame buildings", *Engineering Structures*, 52: 340–354.

CEN – European Committee for Standardization (2006) "Eurocode 0: Basis of Structural Design", Final draft. Brussels.

Collins KR, Stojadinovic B (2000) "Limit states for performance-based design",*12WCEE.*

Constantinou MC, Mokha A, Reinhorn AM (1990) "Teflon Bearings in Base Isolation. II: Modeling", *J. Struct. Eng. ASCE*, Vol. 116, No. 2, 455-474.

Constantinou MC, Papageorgiou A (1990) "Stochastic response of practical sliding isolation systems", *Probabilistic Engineering Mechanics*, 5(1): 27–34.

Cornell CA (1968) "Engineering seismic risk analysis", *Bulletin of the Seismological Society of America*; 58(5): 1583–1606.

Dolsek M (2009) "Incremental dynamic analysis with consideration of modelling uncertainties", *Earthq Eng Struct Dyn.*, 38: 805–25.

ESMD http://www.isesd.hi.is/

Fan FG, Ahmadi G (1990) "Random response analysis of frictional base isolation system", *Journal of Engineering Mechanics*, 116(9): 1881–901.

McKey MD, Conover WJ, Beckman RJ (1979) "A comparison of three methods for selecting values of input variables in the analysis from a computer code", *Technometrics*, 21: 239-45.

Mokha A, Constantinou MC, Reinhorn AM (1990) "Teflon Bearings in Base Isolation. I: Testing", *J. Struct. Eng.* Vol. 116, No. 2, 438-454.

Naeim F, Kelly JM (1999) "Design of Seismic Isolated Structures: From Theory to Practice", *John Wiley & Sons, Inc.*

Nagarajaiah S, Reinhorn AM, Constantinou MC (1991) "3D-Basis: Non Linear Dynamic Analysis of Three-Dimensional Base Isolated Structures: Part II", *Technical Report NCEER-91-0005*, National Center for Earthquake Engeneering Reserch, State University of New York at Buffalo, Buffalo, 1991.

NTC08 (2008) "Norme tecniche per le costruzioni", Gazzetta Ufficiale del 04.02.08, DM 14.01.08, Ministero delle Infrastrutture.

Park YJ, Wen YK, Ang AHS (1986) "Random Vibration of Hysteretic Systems under Bi-Directional Ground Motions", *Earthquake Engng Struct. Dyn* 14:543–557.

Saito T, Kanda J, Kani N (1998) "Seismic reliability estimate of building structures designed according to the current Japanese design code", *Proceedings of the Structural Engineers World Congress (SEWC'98)*

SAP2000. Computers and Structures Inc.: Berkley, CA, 2002.

SEAOC Vision 2000 Committee (1995) " Performance-based seismic engineering", *Report* prepared by Structural Engineers Association of California, Sacramento, CA.

Su L, Ahmadi G, Tadjbakhsh IG (1989) " Comparative study of base isolation systems", *Journal of Engineering Mechanics, ASCE*, 115:1976–92.

Zayas VA, Low SS , Mahin SA (1987) "The FPS earthquake resisting system", *Report No.* CB/EERC-87/01, Earthquake Engineering Research Center, University of California, Berkeley, California.